HIGH PRECISION ELECTROHYDRODYNAMIC PRINTING OF POLYMER ONTO
MICROCANTILEVER SENSORS

BY

JAMES H. PIKUL

THESIS

Submitted in partial fulfillment of the requirements
for the degree of Master of Science in Mechanical Engineering
in the Graduate College of the
University of Illinois at Urbana-Champaign, 2011

Urbana, Illinois

Adviser:

Professor William Paul King

ABSTRACT

This thesis reports electrohydrodynamic jet printing to deposit $2 - 27$ μm diameter polymer droplets onto microcantilever sensors. The polymer droplets were deposited as single droplets or organized patterns, with sub-μm control over droplet diameter and position. The droplet size could be controlled through a pulse-modulated source voltage, while droplet position was controlled using a positioning stage. Gravimetry analyzed the polymer droplets by examining the shift in microcantilever resonance frequency resulting from droplet deposition. The resonance shift of 50 - 4130 Hz corresponded to a polymer mass of 4.5 - 135 pg. The electrohydrodynamic method is a precise way to deposit multiple materials onto micromechanical sensors with greater resolution and repeatability than current methods.

This thesis is dedicated to my family for instilling in me the importance of education and for providing unending support in helping me achieve my dreams. In particular to my Grandmother who sacrificed many things to ensure excellence in my early mathematics and music education. I cannot say enough about the support, knowledge, and friendship I have received from my girlfriend, Rhiannon, whom I dearly love and also dedicate this thesis to.

ACKNOWLEDGMENTS

TABLE OF CONTENTS

CHAPTER 1: INTRODUCTION

Microcantilever sensors are of interest due to their high sensitivity, low cost label-free detection of various analytes, and compatibility with silicon electronics. Microcantilevers are micromechanical spring boards that are anchored at one end and free at the other end. These physical sensors can respond to changes in surface stress or adherent material, which are detected through cantilever bending or frequency change [1] – [5].

Most applications of microcantilever sensors employ a functional layer that coats the cantilever. This functional layer is selected to be sensitive to environmental change or stimulus. Examples of these functional layers include self-assembled monolayers (SAMs), polymers, hydrogels, and biomolecules (DNA, antibodies, polypeptides, and nucleotides) [6]. One of the biggest technical challenges for microcantilever sensors is: how precisely can one deliver this functional material to the cantilever. Precise control of the functional layer location is required for measuring the smallest analyte quantity. For example 50 – 400 nm precision was required to detect 6.3 – 213.1 attograms of thiolate self-assembled monolayer systems [7]. Precise application of functional layers increases the sensitivity of cantilevers [8] – [10], [11], reduces adhesion problems from functional layer expansion [12], and enables detection of multiple analytes on a single cantilever using higher order resonant modes [8] – [10], [13]. When using cantilever resonance to detect changes in mass of an adherent material, the measurement precision depends upon knowing the location of the mass, since the resonant frequency shift changes with mass location [14], [8] – [10].

Polymer functional layers are of particular interest due to their high sensitivity caused by the large differential stress produced from swelling during analyte absorption [15], [16]. Precise

patterning of polymer onto microcantilever sensors enhances sensitivity by amplifying the stress seen in the cantilever [15], in addition to the benefits of controlling the location of adsorbed mass. Polymer functional layers have been incorporated with microcantilever sensors to detect humidity and pH changes [17] – [19], alcohols, alkanes, ethers, aromatics, esters, ketones, nitriles, haloalkanes, solvents, perfume essences, and beverage flavors [20] – [23]. Polymers are also used as inert coverings on reference cantilevers [24], [25].

Multiple cantilevers in an array can detect multiple analytes, which is possible when each cantilever is functionalized with a different functional layer. Recent papers report sensing of 13 different chemicals using arrays of 2 or 6 cantilevers coated with different polymers [22], [23]. Increasing the number of cantilevers in an array increases the number of analytes that can be detected at one time. Integration of multiple polymers onto multiple cantilevers in an array, without cross contamination, is challenging and requires micrometer control over the size and position of the functional layer. Individual cantilevers in arrays can be functionalized with polymer using drop-coating, microarray spotting pins, immersion in capillaries, and inkjet printing [21] – [23], [26]. These techniques are limited to resolutions in the hundreds of micrometers and lack the ability to print patterns or precisely locate polymer onto microcantilever sensors. The best resolution for the deposition of polymers onto microcantilevers is demonstrated with inkjet printing, with droplets of diameter 60 μm and placement precision of 10 μm. The deposition diameter, after contact with the cantilever, is around 100 μm [26].

The precise deposition of polymers onto microcantilever sensors with micrometer resolution and control has become increasingly important as sensors are required to detect more analytes with higher sensitivity. This thesis uses electrohydrodynamic jet (e-jet) printing to deposit 2 – 27 μm diameter droplets of molten polyethylene onto microcantilever sensors. We

demonstrate sub-μm control of droplet diameter and positioning. Using the cantilever resonance, mass of individual droplets is measured to be between 4.5 and 135 pg and the effect of droplet location on cantilever sensitivity is demonstrated.

CHAPTER 2: SYSTEM DESCRIPTION

2.1 Electrohydrodynamic Jet Printing

E-jet printing is a high resolution printing technology where the printed liquid is driven by an electric field [27]. Exposure to an electric field causes mobile ions in a polarizable liquid to accumulate at the liquid surface. The coulombic repulsion of the ions causes the meniscus at the nozzle end to deform into a conical shape, called a Taylor cone. When the electric field exceeds a critical limit, the stress from the surface charge repulsion at the cone apex exceeds the surface tension and a droplet of fluid is emitted towards the grounded substrate. The keys to high resolution droplet printing are to use electric field potentials below those required for atomization mode, or spray mode, as well as the use of small micropipette nozzles with diameters less than 10 μm. Deposited droplets can be as small as 240 nm with spatial accuracy in the hundreds of nm [27]. The deposition rate can be controlled up to 10 kHz with independent droplet size control using a pulse voltage signal [28]. Oligonucleotides, organic and inorganic solutions with conducting polymer, single walled carbon nanotubes, and photocurable pre polymers are printable with e-jet printing [27], [29].

2.2 Experimental Setup

Figure 2.1 shows the e-jet printing setup used in this experiment. Two different sized glass micropipettes, with inner diameter 5 or 10 μm, were filled with molten polyethylene. Polyethylene was chosen due to its low melting temperature and the diversity of applications that use polyethylene. Before filling, the outside of the pipettes were sputter coated with a 15 nm film of gold-palladium that served as the nozzle electrode. The pipette was then inserted into a NiCr

heater, shown in Figure 2.1a, and attached to a syringe. The stabilizer, a clamping system attached to a rigid body, was mounted to the end of the NiCr heater to prevent thermal drift of the micropipette. In addition the substrate was heated to 90 °C using a thermoelectric and the NiCr heater was brought to approximately 120 °C. The relative pressure in the syringe was controlled between zero and thirty pounds per square inch. The target microcantilever was mounted to a 5 – axis controlled stage and positioned 20 – 40 μm below the micropipette tip. When the target area of the cantilever was positioned below the micropipette and a pulse voltage signal was applied between the nozzle electrode and the grounded cantilever, a jet of polymer was deposited as a droplet on the target area of the cantilever, shown in Figure 2.1b. The cantilevers used in this experiment were tipless silicon cantilevers, MikroMasch CSC12. These cantilevers were chosen because they are commercially available tipless cantilevers that have a resonance frequency in the range 50 – 100 kHz, and are appropriately sized to deposit μm sized droplets in various dimensions and configurations. The cantilevers had an aluminum coating on the backside, which served as the electrode for the e-jet process. The exception to the use of these cantilevers was in Figure 3.2, where we deposit droplets onto cantilevers having sharp tips.
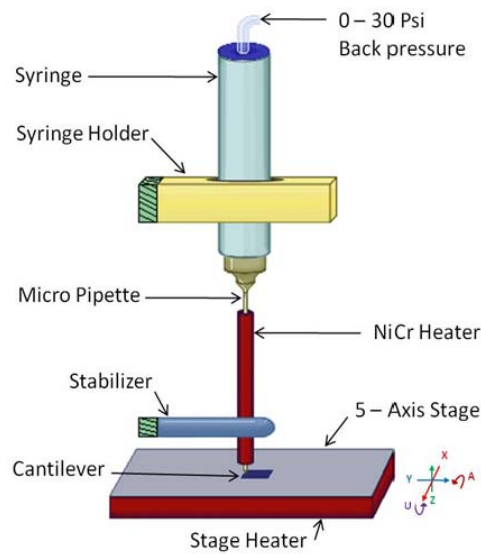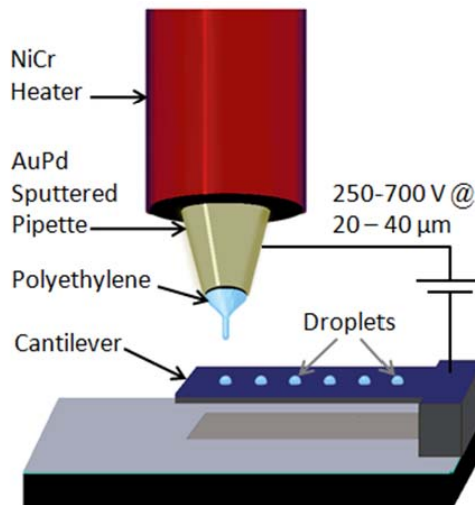
Figure 2.1. The experimental set up used to electrohydrodynamically jet polyethylene onto microcantilevers. (a) An overview of the e-jet printing aparatus consisting of a gold-palladium coated micropipette attached to a syringe with a variable back pressure input. The Syringe is mounted to a rigid body with the syringe holder. Surrounding the micropipette is a NiCr heater used to melt the polyethylene and a stabilizer to reduce thermal drift of the pipette tip. Positioned below the pipette tip is the stage with the target cantilever mounted on top. The stage is heated by a thermoelectric and controlled with a 5 − axis controller. (b) A close up of the micropipette tip in (a) showing the polyethylene with a Taylor cone and being e-jet printed onto a cantilever. The pipette tip and cantilever are separated by 20 − 40 μm and the jetting is performed between 250 and 700 volts using a pulse voltage signal.

6

CHAPTER 3: RESULTS

3.1 Electrohydrodynamic Jet Printing of Polymer onto Microcantilevers

Pure polyethylene was e-jet printed in its molten state. Figure 3.1 shows three lines of 10 μm average diameter polyethylene droplets deposited onto a flat aluminum substrate using e-jet printing. The droplet diameters have 227 nm standard deviation. The droplet diameter and spacing are uniform across all three lines and are similar to those presented in previous e-jet printing work using room temperature liquids [27].
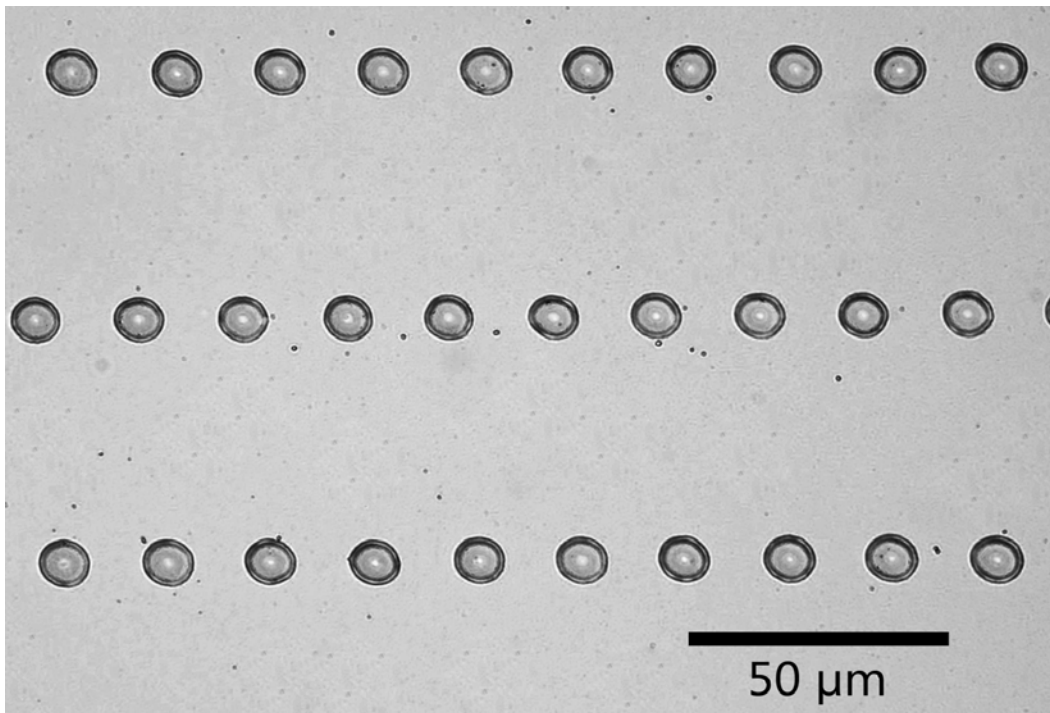

Figure 3.1 Three lines of 10 μm diameter polyethylene droplets deposited onto a flat Aluminum substrate using e-jet printing. The droplet diameter and spacing are uniform across all three lines. The e-jet printing conditions and resulting droplet characteristics are similar to those presented in previous e-jet printing work.

Figure 3.2a shows before and after images of a 27 μm diameter droplet of polyethylene deposited onto a silicon microcantilever. The droplet was formed by depositing several smaller droplets in the same location from the 10 μm micropipette. Figure 3.2b shows a 22 μm diameter droplet of polyethylene deposited onto the tip of a silicon microcantilever.
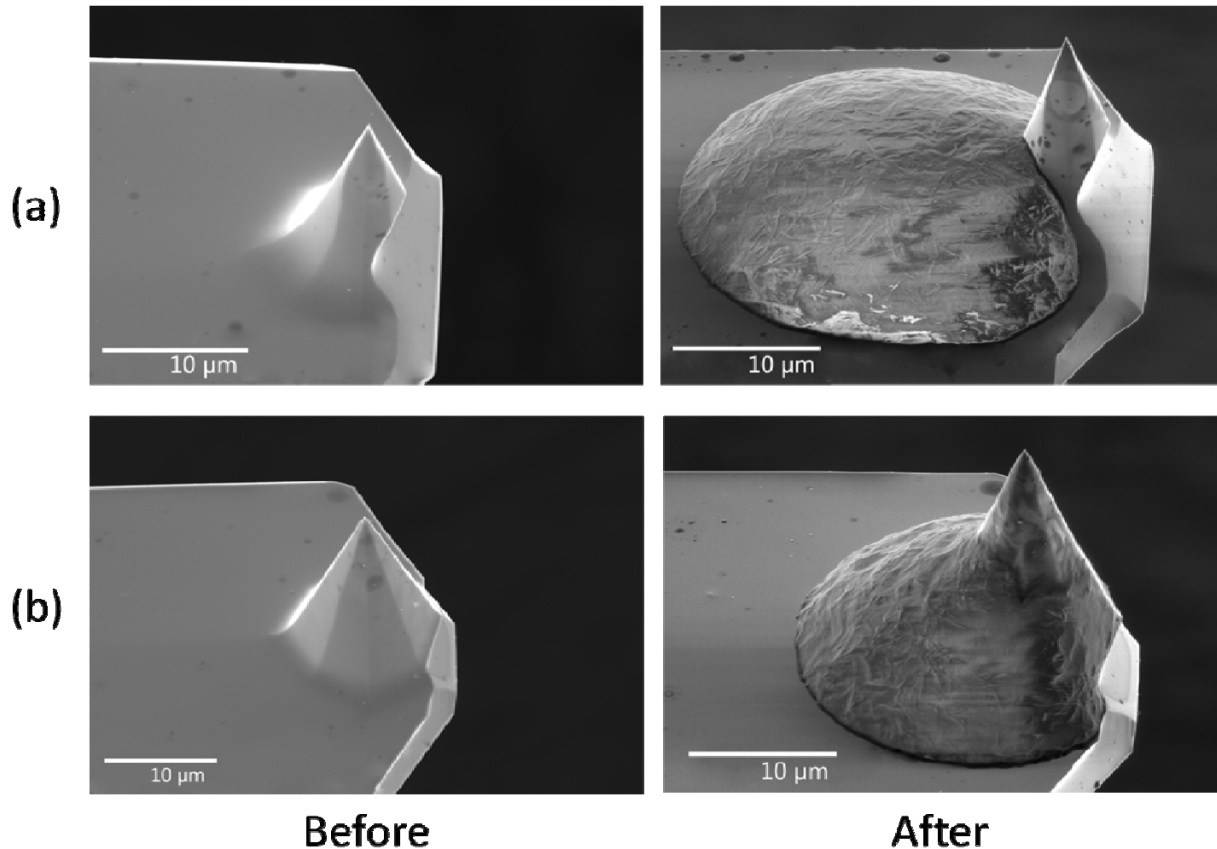

(a)

(b)

Before   **After**

Figure 3.2 Before and after images of polyethylene deposited onto the tips of microcantilevers. (a) A 27 μm diameter droplet of polyethylene deposited onto a tapping mode silicon microcantilever used for imaging in an Atomic Force Microscope. (b) A 22 μm diameter droplet of polyethylene deposited onto the tip of a tapping mode silicon microcantilever. The droplets in (a) and (b) were formed by depositing several droplets in the same location using a 10 μm inner diameter micropipette.

Figure 3.3 shows droplets of polyethylene with various diameters and positions deposited by e-jet printing on tipless silicon cantilevers. Figures 3.3a – d show lines of polyethylene droplets with controlled size and location that progress from a single line with similar sized

droplets to multiple lines with two different sized droplets. Figure 3.3e shows a line of droplets that incrementally increase in diameter from 4 to 18 μms. Figure 3.3f shows a combination of droplets with diameter, position, and spacing changed to further demonstration of control over these parameters. E-jet printing is capable of depositing 2 – 27 μm polyethylene droplets with controlled diameter and position onto microcantilevers.
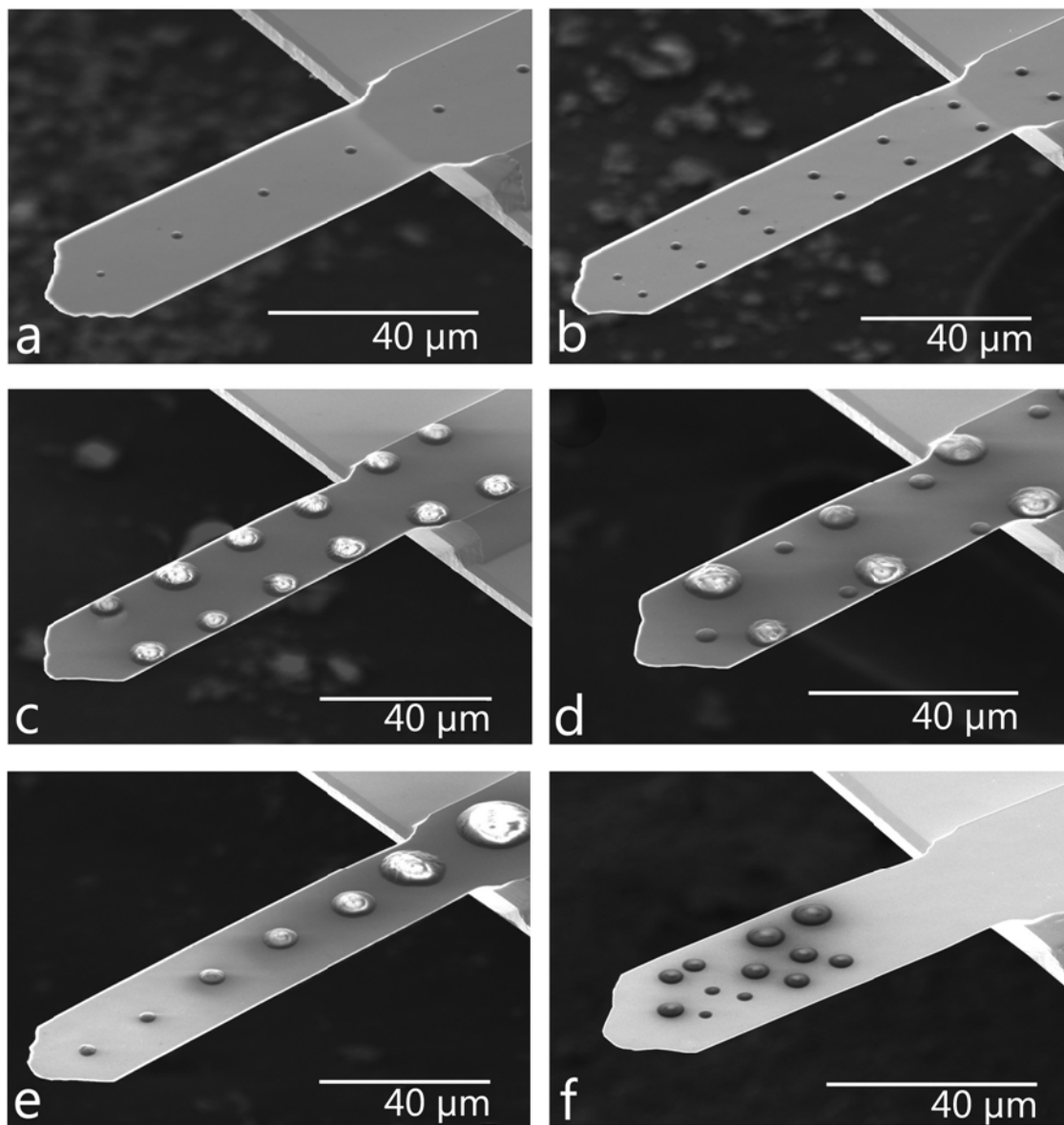

Figure 3.3 (continued on next page)

Figure 3.3 Several tipless microcantilevers with printed patterns of polyethylene that demonstrate the ability to control the diameter and position of droplets deposited onto microcantilevers. (a) A single line of 2 μm diameter droplets printed with a 5 μm pipette. (b) Two parallel lines of 3 μm diameter droplets printed with a 5 μm pipette. (c) Two parallel lines of 9.5 μm average diameter droplets printed with a 10 μm pipette. (d) Two parallel lines of alternating large and small diameter droplets. (e) A single line of deposited droplets that incrementally increase in diameter from 4 to 18 μm. (f) A combination of deposited droplets with changes in diameter, position, and spacing.

3.2 Control of Droplet Size

The sizes of the deposited droplets in Figure 3.3 were controlled by adjusting the voltage applied to the nozzle electrode, separation of the tip and substrate electrodes, back pressure, and selecting the micropipette inner diameter. The voltage necessary to reach the jetting mode of polyethylene was between 250 and 700 volts with a 20 – 40 μm separation between electrodes. For these experiments, a 0.25 Hz pulse voltage signal was used with amplitude 250 – 500 V and duty cycle 0.005 % - 5 %. The duty cycle determined how long the maximum voltage was applied, as a percentage of the pulse signal frequency. At low duty cycles, below 5 %, an increase in duty cycle increased the diameter of a single deposited droplet. Increasing the maximum voltage increased the diameter of a single deposited droplet until a maximum diameter is reached. Individual droplet size is best controlled with either maximum voltage or duty cycle. The limits in droplet size are dependent on the micropipette inner diameter. For 5 μm inner diameter pipettes, a single jetted droplet was limited to sizes between 1 μm and 6.5 μm, or 20 % to 130 % of the diameter opening. A 20 % to 130 % limit is similar for 10 μm inner diameter pipettes. The droplets in Figures 3.3c, d, and e were deposited with a 10 μm inner diameter pipette. The droplets in Figures 3.3a, b, and f were deposited with a 5 μm inner diameter pipette.

The positions of the droplets in Figure 3.3 were placed with sub-μm variance in their location. After an initial droplet was deposited onto a cantilever, each successive droplet was

deposited relative to the previous droplet location. The variances in separation between droplet centers in Figures 3.3a – f, not including d, were less than 0.65 μm in both the distance along the length of the cantilever and across the width. The larger 5 μm variance in spacing for Figure 3.3d is most likely due to larger variation in droplet size from depositing near the cantilever edges, discussed later, and from shifts in the droplet center after depositing multiple droplets in the same location. When comparing the average droplet separation to the droplet separation programmed into the stage, 20 μm along the length and 10 μm along the width in most cases, the variance was less than 0.45 μm for droplets in Figure 3.3 and typically below 100 nm.

3.3 Droplet Shape

Figure 5 shows a side view of the cantilever in Figure 4e where droplets of polyethylene between 4 and 18 um in diameter were deposited. The first two droplets near the cantilever free end were deposited using a single 0.25 Hz voltage pulse with 5 % duty cycle. The sizes of the droplets were controlled by adjusting the maximum voltage applied, between 300 and 450 V. To achieve larger diameter droplets, multiple droplets were printed in the same location. The remaining droplets along the length of the cantilever were deposited with 3, 5, 10, and 15 pulses. A close up of the 1-pulse, 5-pulse, and 15-pulse droplets can be seen at the bottom of Figure 5. The diameters of the droplets are 3.2, 7.3, and 13 μm. The contact angles for each droplet are 30, 49, and 40 degrees.
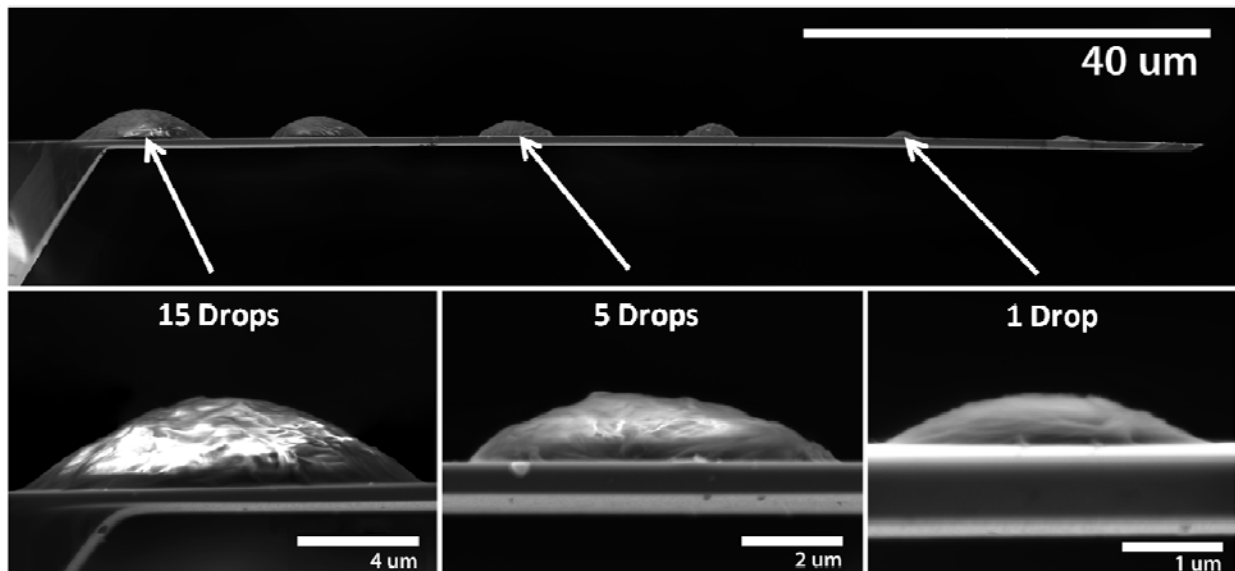
Figure 3.4 A line of 4 to 18 um in diameter polyethylene droplets deposited along the length of a microcantilever. The first two droplets near the free end were deposited using a single pulse. The larger diameter droplets were deposited with 3, 5, 10, and 15 pulses along the length of the cantilever. A close up of the 1 pulse, 5 pulse, and 15 pulse droplets can be seen at the bottom of Figure 5. The diameters of the droplets are 3.2, 7.3, and 13 μm respectively. The contact angles for each droplet are 30, 49, and 40 degrees.

3.4 Variations in Deposition

Changes in electric field across a cantilever can affect the uniformity of the deposited droplets. Two effects occur as polyethylene droplets are deposited near the microcantilever tip. The first effect is a change in electric field line symmetry. The asymmetric electric field lines distort the shape of the Taylor cone and reduce the volume of deposited droplets. The asymmetry is caused by the finite length of the cantilever electrode and defects in the aluminum due to processing. The second effect is a reduction in separation between the cantilever and nozzle. The cantilever deflects due to the electrostatic force between the cantilever and nozzle. The resulting decrease in separation increases the electric field and deposits larger droplets. To achieve uniform droplet

sizes across the length of a cantilever the applied voltage signal can be adjusted to account for changes in the electric field due to cantilever deflection or geometric and material changes.

The thermal drift of the micropipette tip limits the precision of droplet positioning. At room temperature the location of the droplet, determined by the location of the micropipette tip, is limited by the stage resolution of 20 nm. At nozzle temperatures near 200 °C thermal drift reduces placement precision to, at most, a few μm. For the present experiments with polyethylene at 120 °C, the thermal drift is less than a μm during the printing time of one minute and had negligible effect on the droplet positioning.

3.5 Mass Measurements

Mass measurements of various polyethylene droplets deposited onto tipless cantilevers were made by measuring the shift in the cantilever resonant frequency. The spring constant, initial resonant frequency and final resonant frequency of each cantilever were measured using an Asylum MFP-3D AFM. The deflection of the cantilever beam due to thermal noise, in room temperature air, was measured optically to determine the resonant frequency. Figure 3.5 shows the measured cantilever frequency and frequency shift due to added mass. The measured spring constants of the cantilevers were $0.17 - 0.57$ N/m. Neglecting damping, the resonance frequency of a cantilever, f, is [30]

$$f = \frac{1}{2\pi} \sqrt{\frac{K}{m_{eff} + 0.24\, m_c}} \qquad (1)$$

Where K is the cantilever spring constant, m_c is the mass of the cantilever, and the effective deposited mass, m_{eff}, depends on the location of the loaded mass by [8]

$$m_{eff} = m_d \left(\frac{l-x}{l}\right)^3 \qquad\qquad (2)$$

In which m_d is the actual loaded mass, l is the length of the cantilever, and x is the distance of the mass from the free end of the cantilever. Using Equations 1 and 2, the loaded mass on a cantilever with known spring constant can be determined by measuring the change in resonant frequency and location of the deposited droplet.
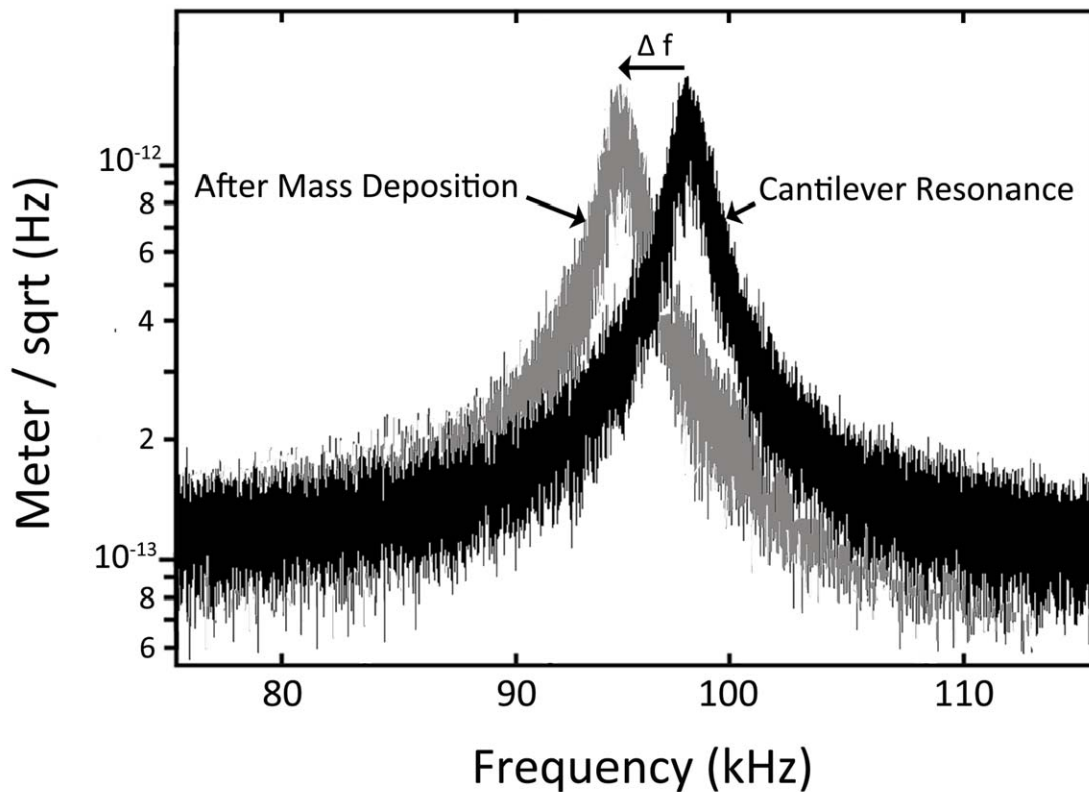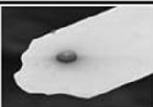

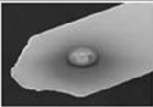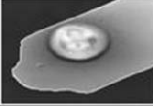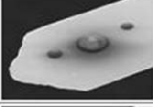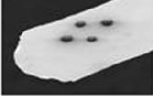**Figure 3.5** A plot of the resonant frequency of a cantilever using an Asylum MFP-3D atomic force microscope. The plot is zoomed in between 80 and 110 kHz to best view the resonant peak and frequency data. The darker peak is the frequency data for the cantilever before deposition. After deposition of polyethylene, the resonant frequency shifts to a lower frequency resulting in the lighter peak.

Table 3.1 shows gravimetry data for five different deposited droplets of polyethylene on five different microcantilevers. The resonant frequency of each cantilever before deposition was indicated by f_o. Δf and m_d indicate the resulting change in resonant frequency of the cantilever and added mass due to the deposited polyethylene droplet. The five droplets had a mass of 4.5, 21.4, 134.5, 23.8, and 10.8 pg. The last column shows images of each droplet deposited on the cantilevers. It is possible to estimate the size of the droplets using scanning electron microscopy, and from the known density of polyethylene (0.92 g / cm^3) estimate the droplet mass. The mass of the droplets are estimated as 7.82, 36.22, 220.38, 39.56, and 11.28 pg. The accuracy of this droplet mass estimation is limited by the microscopy resolution and inaccuracy in the volume calculation due to the complex droplet shapes. In addition the density of the polyethylene at the scale of the deposited droplets is not known. Overall, we have higher confidence in the cantilever-based mass measurement than the estimate from SEM.

Table 3.1 Gravimetry Results

Droplet	f_o [KHz]	Δf [Hz]	m_d [pg]	Image
1	99.024	153	4.50	
2	91.309	663	21.40	
3	98.669	4128	134.50	
4	73.498	387	23.80	
5	53.332	50	10.80	

In order to test the effect of droplet location on the change in cantilever resonant frequency, three polyethylene droplets were consecutively deposited at different distances from the microcantilever tip. Figure 3.6 shows the sequence of deposited droplets. The resonant frequency of the clean cantilever was measured and a 6.5 μm diameter droplet was deposited 14 μm from the free end, seen in Figure 3.6a. The cantilever was then removed from the e-jet printing apparatus and the resonant frequency was measured, with a corresponding shift of 466 Hz. Using the same voltage signal and heating conditions as the first deposition, a second droplet of polyethylene was deposited 32 μm from the free end, shown in Figure 3.6b. The droplet had diameter 6.1 μm which induced a change in resonant frequency of 121 Hz. The final droplet was deposited 49 μm from the free end under the same conditions and had a 5.4 μm diameter and induced a frequency change of 63 Hz, seen in Figure 3.6c. Table 3.2 shows the corresponding mass of each droplet, change in frequency, distance from free end, diameter, and Δf / Δm. The sensitivity of a cantilever is increased if a small change in added mass, Δm, results in a large change in the frequency shift, Δf. The droplet deposited closest to the free end, droplet 1, has a Δf / Δm 21X greater than droplet deposited near the cantilever base, droplet 3. The sensitivity of a cantilever gravimeter, to a change in mass, increases when the mass is precisely added to the free end of the micro cantilever.

16
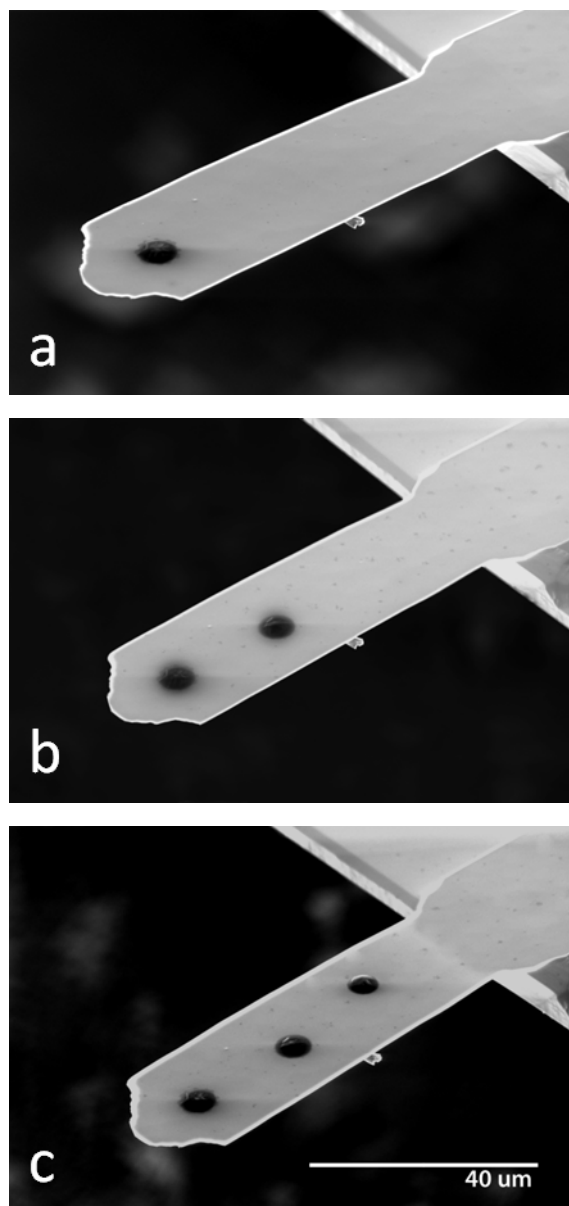
Figure 3.6 A sequence of polyethylene droplets deposited consecutively onto a microcantilever. After each deposition the cantilever was removed from the e-jet printing apparatus and the resonant frequency was measured. The corresponding mass of each droplet, change in frequency, distance from free end, and diameter are shown in Table 3.2.

Table 3.2 Consecutive Cantilever Loading

	Droplet 1	Droplet 2	Droplet 3
Δf [Hz]	466	121	63
Distance from end (x) [μm]	14	32	49
m_d [pg]	11	10	30
Diameter of droplet (D) [μm]	6.5	6.1	5.4
$\Delta f / \Delta m$	42	12	2

CHAPTER 4: CONCLUSIONS

4.1 Applications

New sensor platforms that detect multiple analytes on one microcantilever can utilize e-jet printing to deposit multiple functional materials onto specific locations. The high resolution of the e-jet printing technique would eliminate cross contamination when depositing functional material onto arrays of microcantilevers. Precise patterning of polymer onto microcantilever sensors can be used to enhance the cantilever sensitivity by patterning the polymer in geometries that amplify the stress seen in the cantilever [15]. The e-jet printing technique can be applied to print polymer onto cantilever tips for tip-based manufacturing [31], [32]. In addition it can be used to print polymer in organic electronics, novel material fabrication, and onto micromechanical devices used in nanofabrication and material characterization.

4.2 Future work

Perhaps the most promising direction for future work in depositing molten material utilizing e-jet printing is applying the technique to deposit insulators, conductors, and semi-conductors for printable electronics. Low melting temperature glass, metals, and semi-conducting polymers could be printed to fulfill the roles of insulators, conductors, and semi-conductors. The ability to print this diverse set of materials would open opportunities for electronics that can be printed on flexible polymers, paper, and silicon in ambient environments, eliminating the need for clean room processing.

E-jet printing has been used to print biological materials such as DNA and oligonucleotides [27], [29]. Future work on printing these materials onto microcantilever sensors could open up interesting opportunities for specifically functionalizing biological sensors.

4.3 Summary

Electrohydrodynamic jet printing of molten polymer was used to print droplets of polyethylene, with μm-scale control of droplet diameter and positioning, onto microcantilever gravimetric sensors. The deposited droplet diameters ranged in size from $2 - 27$ μm. The polymer droplets were deposited as single droplets or organized patterns, with sub-μm control over droplet diameter and position. The droplet size could be controlled through a pulse-modulated source voltage, while droplet position was controlled using a positioning stage. Using the change in resonance frequency of the microcantilevers, the mass of the deposited droplets were measured to be between 4.5 - 135 pg.

REFERENCES

[1] N. V. Lavrik, M. J. Sepaniak, and P. G. Datskos, "Cantilever transducers as a platform for chemical and biological sensors," Rev. Sci. Instr., vol. 75, no. 7, pp. 2229–2253, July 2004.

[2] T. Thundat, R. J. Warmack, G. Y. Chen, and D. P. Allison, "Thermal and ambient-induced deflections of scanning force microscope cantilevers," Appl. Phys. Lett., vol. 64, no. 21, pp. 2894–2896, May 1994.

[3] R. Raiteri, M. Grattarola, H. J. Butt, and P. Skladal, "Micromechanical cantilever-based biosensors," Sensor. Actuat. B–Chemical, vol. 79, pp. 115–126, 2001.

[4] C. Ziegler, "Cantielver-based biosensors," Anal. Bioanal. Chem., vol. 379, pp. 946–959, 2004.

[5] P. S. Waggoner, and H. G. Craighead, "Micro- and nanomechanical sensors for environmental, chemical, and biological detection," Lab Chip, vol. 7, pp. 1238–1255, 2007.

[6] S. Singamaneni, M. C. LeMieux, H. P. Lang, C. Gerber, Y. Lam, S. Zauscher, P. G. Datskos, N. V. Lavrik, H. Jiang, R. R. Naik, T. J. Bunning, and V. V. Tsukruk, "Bimaterial microcantilevers as a hybrid sensing platform," Adv. Mater., vol. 20, pp.653–680, 2008.

[7] B. Ilic, H. G. Craighead, S. Krylov, W. Senaratne, C. Ober, and P. Neuzil, "Attogram detection using nanoelectromechanical oscillators," J. Appl. Phys., vol. 95, no. 7, pp. 3694–3703, April 2004.

[8] S. Dohn, S. Schmid, F. Amiot, and A. Boisen, "Position and mass determination of multiple particles using cantilever based mass sensors," Appl. Phys. Lett., vol. 97, no. 044103, pp. 1–3, 2010.

[9] S. Dohn, R. Sandberg, W. Svendsen, and A. Boisen, "Enhanced functionality of cantilever based mass sensors using higer modes," Appl. Phys. Lett., vol. 86, no. 233501, pp. 1–3, 2005.

[10] H. Xie, J. Vitard, S. Haliyo, and S. Regnier, "Enhanced sensitivity of mass detection using the first torsional mode of microcantilevers," Meas. Sci. Technol., vol. 19, no. 055207, pp. 1–7, 2008.

[11] V. Toffoli, F. Esch, M. Melli, F. Cataruzza, A. Pozzato, S. Carrato, G. Scoles, M. Tormen, and M. Lazzarino, "Intrinsically alsigned chemo-mechanical functionalization of twin cantilever structures," Nanotechnology, vol. 19, pp. 7–13, 2008.

[12] Y. I. Chou, H. C. Chiang, and C. C. Wang, "Study on Pd functionalization of microcantilever for hydrogen detection promotion," Sensor. Actuat. B–Chemical, vol. 129, pp. 72–78, 2008.

[13] H. Yu and X. Li, "Bianalyte mass detection with a single resonant microcantilever," Appl. Phys. Lett., vol. 94, no. 011901, pp. 1 – 3, 2009.

[14] J. E. Sader, I. Larson, P. Mulvaney, and L. R. White, "Method for the calibration of atomic force microscope cantilevers," Rev. Sci. Instrum., vol. 66, no. 7, 1995.

[15] N. L. Privorotskaya and W. P. King, "The mechanics of polymer swelling on microcantilever sensors," Microsyst. Technol., vol. 15, pp. 333–340, 2009.

[16] M. R. Begley, M. Utz, and U. Komaragiri, "Chemo-mechanical interactions between adsorbed molecules and thin elastic films," J. Mech. Phys. Solids, vol. 53, pp. 2119–2140, 2005.

[17] T. Thundat, G. Y. Chen, R. J. Warmack, D. P. Allison, and E. A. Wachter, "Vapor detection using resonating microcantilevers," Anal. Chem., vol. 67, pp. 519–521, 1995.

[18] J. Gonska, C. Schelling, and G. Urban, "Application of hydrogel-coated microcantilevers as sensing elements for pH," J. Micromech. Microeng., vol. 19, no. 127002, pp. 1–8, 2009.

[19] R. Bashir, J. Z. Hilt, O. Elibol, A. Gupta, and N. A. Peppas, "Micromechanical cantilever as an ultrasensitive pH microsensor," Appl. Phys. Lett., vol. 81, no. 6, pp. 3091–3093, Oct. 2002.

[20] F. M. Battiston, J. P. Ramseyer, H. P. Lang, M. K. Baller, C. Gerber, J. K. Gimzewski, E. Meyer, and H. J. Güntherodt, "A chemical sensor based on a microfabricated cantilever array with simultaneous resonance-frequency and bending readout," Sens. Actuat. B–Chem, vol. 77, pp. 121–131, 2001.

[21] H. P. Lang, J. P. Ramseyer, W. Grange, T. Braun, D. Schmid, P. Hunziker, C. Jung, M. Hegner, and C. Gerber, "An artificial nose based on microcantilever array sensors," J. Phys.: Conf. Ser., vol. 61, pp. 663–667, 2007.

[22] A. Loui, T. V. Ratto, T. S. Wilson, S. K. McCall, E. V. Mukerjee, A. H. Love, and B. R. Hart, "Chemical vapor discrimination using a compact and low-power array of piezoresistive microcantilevers," Analyst, vol. 133, pp. 608–615, 2008.

[23] M. Li, E. B. Myers, H. X. Tang, S. J. Aldridge, H. C. McCaig, J. J. Whiting, R. J. Simonson, N. S. Lewis, and M. L. Roukes, "Nanoelectromechanical resonantor arrays for ultrafast, gas-phase chromatographic chemical analysis," Nano Lett., DOI: 10.1021 /nl101586s.

[24] W. Shu, S. Laurenson, T. P.J. Knowles, P. K. Ferrigno, and A. A. Seshia, "Highly specific label-free protein detection from lysed cells using internally referenced microcantilever sensors," Biosensors & Bioelectronics, vol. 24, pp. 233–237, 2008.

[25] D. A. Raorane, M. D. Lim, F. F. Chen, C. S. Craik, and A. Majumdar, "Quantitative and label-free technique for measuring protease activity and inhibition using a microfluidic cantilever array," Nano Lett., vol. 8, no. 9, pp. 2968–2974, 2008.

[26] A. Bietsch, J. Zhang, M. Hegner, H. P. Lang, and C. Gerber, "Rapid functionalization of cantilever array sensors by inkjet printing," Nanotechnology, vol. 15, pp. 873–880, 2004.

[27] J. Park, M. Hardy, S. J. Kang, K. Barton, K. Adair, D. K. Mukhopadhyay, C. Y. Lee, M. S. Strano, A. G. Alleyne, J. G. Georgiadis, P. M. Ferreira, and J. A. Rogers, "High-resolution electrohydrodynamic jet printing," Nat. Mater., vol. 6, pp. 782–789, Oct. 2007.

[28] S. Mishra, K. Barton, A. Alleyne, P. Ferreira, and J. Rogers, "High speed drop-on-demand printing with a pulsed electrohydrodynamic jet," J. Micromech. Microeng., vol. 20, no. 9, 2010.

[29] J. Park, J. H. Lee, U. Paik, Y. Lu, and J. A. Rogers, "Nanoscale patterns of oligonucleotides formed by electrohydrodynamic jet printing with applications in biosensing and nanomaterials assembly," Nano Lett., vol. 8, no. 12, pp. 4210–4216, 2008.

[30] J. P. Cleveland, S. Manne, D. Bocek, and P. K. Hansma, "A nondestructive method for determining the spring constant of cantilevers for scanning force microscopy," Rev. Sci. Instrum., vol. 64, no. 2, 1993.

[31] P. E. Sheehan, L. J. Whitman, W. P. King, and B. A. Nelson, "Nanoscale deposition of solid inks via thermal dip pen nanolithography," Appl. Phys. Lett., vol. 85, no. 9, Aug. 2004.

[32] P. C. Fletcher, J. R. Felts, Z. Dai, T. D. Jacobs, H. Zeng, W. Lee, P. E. Sheehan, J. A. Carlisle, R. W. Carpick, and W. P. King, "Wear-resistant diamond nanoprobe tips with integrated silicon heater for tip-based nanomanufacturing," ACS Nano, vol. 4, no. 6, pp. 3338–3344, 2010.